Evolution of Enzymatic Activity in the Enolase Superfamily: Structural and Mutagenic Studies of the Mechanism of the Reaction Catalyzed by *o*-Succinylbenzoate Synthase from *Escherichia coli*[†,‡]

Vadim A. Klenchin,[§,‖] Erika A. Taylor Ringia,[‖,⊥] John A. Gerlt,*,[⊥] and Ivan Rayment*,[§]

Departments of Chemistry and Biochemistry, University of Illinois, Urbana, Illinois 61801, and Department of Biochemistry, University of Wisconsin, Madison, Wisconsin 53705

Received August 28, 2003; Revised Manuscript Received October 17, 2003

ABSTRACT: *o*-Succinylbenzoate synthase (OSBS) from *Escherichia coli*, a member of the enolase superfamily, catalyzes an exergonic dehydration reaction in the menaquinone biosynthetic pathway in which 2-succinyl-6-hydroxy-2,4-cyclohexadiene-1-carboxylate (SHCHC) is converted to 4-(2′-carboxyphenyl)-4-oxobutyrate (*o*-succinylbenzoate or OSB). Our previous structural studies of the Mg^{2+}·OSB complex established that OSBS is a member of the muconate lactonizing enzyme subgroup of the superfamily: the essential Mg^{2+} is coordinated to carboxylate ligands at the ends of the third, fourth, and fifth β-strands of the $(\beta/\alpha)_7\beta$-barrel catalytic domain, and the OSB product is located between the Lys 133 at the end of the second β-strand and the Lys 235 at the end of the sixth β-strand [Thompson, T. B., Garrett, J. B., Taylor, E. A, Meganathan, R., Gerlt, J. A., and Rayment, I. (2000) *Biochemistry 39*, 10662−76]. Both Lys 133 and Lys 235 were separately replaced with Ala, Ser, and Arg residues; all six mutants displayed no detectable catalytic activity. The structure of the Mg^{2+}·SHCHC complex of the K133R mutant has been solved at 1.62 Å resolution by molecular replacement starting from the structure of the Mg^{2+}·OSB complex. This establishes the absolute configuration of SHCHC: the C1−carboxylate and the C6−OH leaving group are in a *trans* orientation, requiring that the dehydration proceed via a *syn* stereochemical course. The side chain of Arg 133 is pointed out of the active site so that it cannot function as a general base, whereas in the wild-type enzyme complexed with Mg^{2+}·OSB, the side chain of Lys 133 is appropriately positioned to function as the only acid/base catalyst in the *syn* dehydration. The ϵ-ammonium group of Lys 235 forms a cation−π interaction with the cyclohexadienyl moiety of SHCHC, suggesting that Lys 235 also stabilizes the enediolate anion intermediate in the *syn* dehydration via a similar interaction.

The members of the enolase superfamily catalyze mechanistically diverse reactions initiated by the abstraction of a proton from a carbon adjacent to a carboxylate group (α-proton) by an active site base to generate an enediolate anion intermediate. This intermediate, which is stabilized by coordination to an essential Mg^{2+} ion, is then processed to the product by an active site acid (*1*). The members of the superfamily share a two-domain structure, with the active sites located at their interface. The larger central domain consists of a $(\beta/\alpha)_7\beta$-barrel domain and encompasses the three ligands for the Mg^{2+} at the ends of the third, fourth, and fifth β-strands as well as one or more acid/base catalysts at the C-terminal ends of the second, third, fifth, sixth, or seventh β-strands. The smaller capping domain, which exhibits a mixed α/β motif, is more variable and is formed from both the N- and the C-termini of the polypeptide. This domain typically contains residues involved in substrate binding.

Excluding the ubiquitous enolases, over 500 nonredundant members of the superfamily now can be identified in the sequence databases (J. A. Gerlt, unpublished observations). These can be partitioned into two groups based on the identities of the acid/base catalysts. The mandelate racemase (MR)[1] subgroup is defined by a conserved His-Asp dyad, with the His and Asp residues located at the C-terminal ends
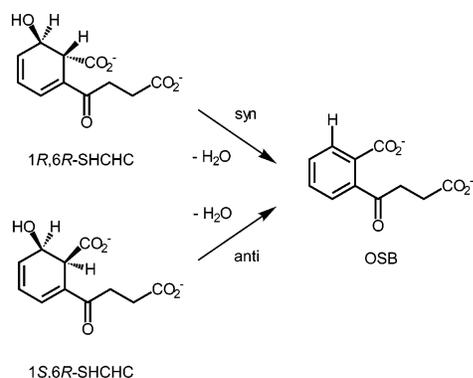
* To whom correspondence should be addressed. (I.R.) Phone: (608) 262-0437. Fax: (608) 262-1319. E-mail: Ivan_Rayment@biochem.wisc.edu. (J.A.G.) Phone: (217) 244-7414. Fax: (217) 244-6538. E-mail: j-gerlt@uiuc.edu.
§ University of Wisconsin.
‖ These two authors contributed equally to this work.
⊥ University of Illinois.

[1] Abbreviations: APS, Advanced Photon Source at Argonne National Laboratory; MePEG, methyl ether poly(ethylene glycol); MLE, muconate lactonizing enzyme; MR, mandelate racemase; OSBS, *o*-succinylbenzoate synthase; SBC, The Structural Biology Center at the Advanced Photon Source, Argonne, IL; SHCHC, 2-succinyl-6-hydroxy-2,4-cyclohexadiene-1-carboxylate; OSB, 4-(2′-carboxyphenyl)-4-oxobutyrate or *o*-succinylbenzoate; rms, root-mean-square; rmsd, root-mean-square deviation.

Scheme 1 : Conversion of SHCHC to OSB Catalyzed by
o-Succinylbenzoate Synthase

Scheme 2 : Enzymatic Synthesis of SHCHC from
Chorismate

6*R* in SHCHC); however, the absolute configuration of C1
bearing the α-proton is established in the reaction catalyzed
by SHCHC synthase and has not been experimentally
determined.

In this paper, we establish that OSBS from *E. coli*
catalyzes a *syn* dehydration reaction. Replacements of either
Lys 133 or Lys 235 with Ala, Ser, or Arg residues yield
proteins with no detectable catalytic activity. We solved the
structure of the $Mg^{2+} \cdot$ SHCHC complex of the K133R
mutant, thereby allowing the configuration of the substrate
to be established. The 6-OH leaving group and the 1-car-
boxylate group are *trans* substituents of the C1−C6 bond,
requiring that the dehydration reaction proceed via a *syn*
stereochemical course. The inactivity of the K133R mutant
is attributed to the inability of the Arg 133 side chain to fit
in the active site, so it extends away from the bound SHCHC
and cannot abstract the α-proton. The ε-ammonium group
of Lys 235 forms a cation−π interaction with the cyclo-
hexadienyl moiety of SHCHC, thereby providing the op-
portunity for enhanced stabilization of an enediolate anion
intermediate. Such assistance in catalysis is a novel catalytic
role for an active site functional group in the enolase
superfamily.

MATERIALS AND METHODS

E. coli strains XL1-Blue and BL-21 (DE3) were obtained
from Stratagene. Taq DNA polymerase and restriction
enzymes were purchased from Invitrogen. Oligonucleotide
primers were synthesized by Operon (Alameda, CA) or by
Biosynthesis (Lewisville, TX). Deuterated reagents were
obtained from Cambridge Isotopes Ltd. All other reagents
were of the highest quality grade commercially available.

NMR spectra were recorded using Varian Unity Inova 500
and 600 MHz NMR spectrometers. Spectrophotometric
assays were performed with a Perkin-Elmer Lambda-14
spectrophotometer. PCR reactions were performed using a
MJ Research PTC-200 Peltier Thermal Cycler.

*Biosynthesis of 2-Succinyl-6-hydroxy-2,4-cyclohexadiene-
1-carboxylate (SHCHC).* SHCHC was synthesized from
barium chorismate, α-ketoglutarate (α-KG), thiamin diphos-
phate (TDP), and the coupled actions of isochorismate mutase
(encoded by the *entC* gene from *E. coli*) and SHCHC
synthase (encoded by the *menD* gene from *E. coli*) and
purified as described previously (*4*). ESI-MS 247.1 (corre-
sponds to monolithiated, monoprotonated species); $\lambda_{max} =$
298 nm, $\epsilon = 4000$ M^{-1}; HPLC elution time from a C8
reverse phase column with isocratic elution with 95% of an
aqueous solution of 0.1% TFA, 5% acetonitrile, ~7 min;
^{1}H NMR (500 MHz, ^{2}H$_2$O) δ2.29 (m, 2H), δ2.91 (m, 2H),
δ3.58 (d, 1.6 Hz, 1H), δ4.42 (dd, 1.7, 5.4 Hz, 1H), δ6.18
(dd, 5.4, 9.3 Hz, 1H), δ6.25 (dd, 5.7, 9.5 Hz, 1H), δ7.16(d,
5.7 Hz, 1H).

of the seventh and sixth β-strands, respectively. In addition,
many, but not all members of this subgroup contain a Lys-
X-Lys motif at the end of the second β-strand. The muconate
lactonizing enzyme subgroup is defined by both a conserved
Lys-X-Lys motif at the end of the second β-strand as well
as a Lys at the end of the sixth β-strand. The C-terminal
ends of the second and sixth/seventh β-strands are located
on opposite faces of the active site, so these can catalyze
α-proton abstraction and delivery in reactions proceeding
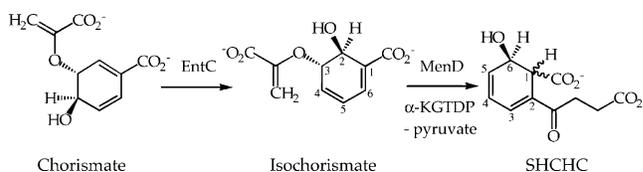by either *syn* or *anti* stereochemical courses.

o-Succinylbenzoate synthases (OSBSs) are members of
the MLE subgroup and catalyze an exergonic dehydration
reaction in which 2-succinyl-6-hydroxy-2,4-cyclohexadiene-
1-carboxylate (SHCHC) is converted to 4-(2′-carboxy-
phenyl)-4-oxobutyrate (*o*-succinylbenzoate or OSB) (Scheme
1).

An abundant number of sequences for OSBSs is available
(>70) since this enzyme is required for the biosynthesis of
menaquinone (*2*), an essential cofactor for anaerobic growth
in eubacteria and some archaea. Although these are highly
diverged, with pairwise sequence identities often <15%,
virtually all orthologs are predicted to contain a Lys-X-Lys
motif at the end of the second β-strand and a Lys at the end
of the sixth β-strand. In the case of the OSBS from
Escherichia coli, this active site architecture has been
confirmed by our structural studies of a complex with $Mg^{2+} \cdot$
OSB that show that the carboxylate group of OSB is
coordinated to the Mg^{2+} and the α-carbon is sandwiched
between the ε-ammonium groups of Lys 133 at the end of
the second β-strand and Lys 235 at the end of the sixth
β-strand (*3*).

Despite the availability of a high-resolution structure for
the $Mg^{2+} \cdot$OSB complex, the mechanism of the OSBS-
catalyzed reaction is uncertain. In particular, the configuration
of the α-carbon of the SHCHC substrate is unknown, thereby
confounding a detailed understanding of the roles of Lys 133
and Lys 235 in catalysis. Without this knowledge, the
stereochemical course, *syn* or *anti*, of the dehydration reaction
likewise cannot be defined (Scheme 1). SHCHC is prepared
enzymatically from chorismate by the coupled actions of
isochorismate synthase and SHCHC synthase (*4*), the latter
a thiamin diphosphate (TDP)-dependent enzyme that uses
isochorismate and α-ketoglutarate (α-KG) as substrates
(Scheme 2).

The configuration of C6 that bears the OH-leaving group
is unchanged from that in isochorismate (2*S* in isochorismate,

Site-Directed Mutagenesis. The template for mutagenesis was the 0.96 kb *menC* gene from *E. coli* MG1655 subcloned using *NdeI* and *XhoI* cloning sites into a modified, 10 histidine-tagged pET15-b vector. The QuikChange site-directed mutagenesis method was utilized to introduce the desired mutations. The mutations were confirmed by sequencing performed at the W. M. Keck Biotechnology Center (Urbana, IL).

Protein Expression and Purification. Mutant proteins of OSBS were expressed in *E. coli* strain BL-21 (DE3) and purified as described previously for the wild-type enzyme (*3*). Fractions containing protein were identified by OD_{280} and SDS−PAGE. Electrospray ionization mass spectrometry (ESI-MS) was used to confirm the expected masses: predicted, 37 736; observed, 37 718 (within the expected 0.1% error).

Circular Dichroism. Wild-type and mutant versions of OSBS were subjected to circular dichroism (CD) studies at the Laboratory of Fluorescence Dynamics at the University of Illinois. The various proteins were dialyzed against 50 mM Tris-HCl, pH 8.0, containing 0.1 mM $MnCl_2$; the samples were adjusted to protein concentrations of ∼0.3 mg/mL. The CD spectra were obtained with a Jasco 720 spectropolarimeter using 0.1 cm quartz (QS) cuvettes. The samples were scanned five times at room temperature over the 190−350 nm wavelength range (0.5 nm increments), and the scans were averaged. The CD spectra were recorded in the absence of any ligands.

Spectrophotometric Assay. OSBS activity was measured at 25 °C using varying concentrations of 2-hydroxyl-6-succinyl-2,4-cyclohexadiene (SHCHC), 50 mM Tris-HCl, pH 8.0, and 0.1 mM $MnCl_2$ by quantitating the decrease in absorbance at 310 nm ($\Delta\epsilon = -2400$ M^{-1} cm^{-1}).

Kinetic Studies using ^{1}H NMR Spectroscopy. Wild-type and mutant proteins were exchanged into D_2O using an Amicon stirred cell. A 10 mL aliquot of protein was concentrated to 2 mL; 8 mL of D_2O was added, and the protein solution was again concentrated to 2 mL. This process was repeated three times. Samples for ^{1}H NMR analysis (800 μL) contained 1 mM SHCHC, 0.5 mg of protein, 50 mM $[d_{11}]$-Tris-DCl, pD 8.0, and 0.1 mM $MnCl_2$ in D_2O. Samples were monitored for formation of the OSB product as well as exchange of the α-proton of the SHCHC substrate at 0, 24, and 48 h. Kinetic studies using ^{1}H NMR spectroscopy (600 MHz) were performed at 25 °C.

Crystallization and X-ray Data Collection. The K133R mutant of OSBS was concentrated to 15 mg/mL, dialyzed against 5 mM Tris-HCl, pH 8.3 containing 2 mM $MgCl_2$, drop frozen as small pellets in liquid nitrogen, and stored at −80 °C. Crystals were grown at 20 °C by small-scale batch experiments by combining 15 μL of protein solution and 15 μL of a solution containing 12−13% MePEG 5000, 100 mM sodium acetate, 60 mM $MgCl_2$, at pH 5.5 (*5*). SHCHC was included in the crystallization at a final concentration of approximately 2.5 mM. These conditions were similar to those used to obtain the structure of the product complex (*3*). Crystals grew spontaneously on occasions but were generally grown by streak seeding 24 h after mixing. Typically, the crystals attained a maximum size of ∼0.5 × 0.5 × 0.05 mm after two weeks. They belong to space group $P2_12_12$ with cell dimensions of $a = 72.1$, $b = 82.9$, and $c =$

Table 1: Data Collection and Refinement Statistics

space group	$P2_1P2_1P2$
unit cell, Å	$a = 72.2$, $b = 82.9$, $c = 56.2$
wavelength, Å	0.979
resolution, Å	31.3−1.62
total reflections	307914
unique reflections	43694
redundancy	7.05
average I/σ (raw/scaled)	41.0/17.1
completeness, %[a]	99.8 (99.9)
R_{merge}, %[b]	4.6 (29.3)
Refinement and Model Statistics	
no. of protein atoms	2484
no. of heteroatoms[c]	361
R factor, %	16.7 (19.5)
R_{free} factor, %	20.0 (24.6)
Wilson B value, Å²	25.9
average B factor, Å²	17.9
Ramachandran, %	
most favored	92.5
additionally allowed	7.5
disallowed	0
rmsd in bond distance, Å	0.016
rmsd in bond angle, °	1.62
disordered side chains	Arg20, Arg22, Ala38, Pro125, Gly126, Glu127

[a] The value in parentheses give the statistics for the highest resolution shell that extends from 1.68 to 1.62 Å. [b] $R_{merge} = (\sum|I_{hkl} - I|/(\sum I_{hkl})100$, where the average intensity I is taken over all symmetry equivalent measurements, and I_{hkl} is the measured intensity for a given reflection. [c] These include 343 water molecules, one molecule of SHCHC, and one magnesium ion.

56.2 Å with a monomer in the asymmetric unit and diffracted to at least 1.6 Å resolution.

Crystals grown in the presence of SHCHC were transferred to a cryo-protectant solution containing 20% MePEG 5000, 15% ethylene glycol, 100 mM $MgCl_2$, 5 mM SHCHC and then were flash-frozen in liquid nitrogen. Initially, the crystals were equilibrated in 20% MePEG 5000, 100 mM $MgCl_2$, 5 mM SHC and then transferred to the final solution in four equal steps of increasing ethylene glycol concentration.

A native data set was recorded at BioCARS beam line 14BM-D at the Advanced Photon Source, Argonne National Laboratory with a single scan composed of 270 frames each of width 0.7° with an exposure of 20 s/frame at a wavelength of 0.979 Å. The data were integrated and scaled with HKL2000 and Scalepack (*6*) (Table 1).

Structure Determination and Refinement. The structure was determined by molecular replacement with the program MOLREP starting from the coordinates for the product complex (PDB accession code 1FHV, ref *3*). Thereafter, the structure was refined with the program Refmac (*7*, *8*). Water molecules were added to the coordinate set with ARP/wARP and subsequent manual verification (*7*, *9*). Iterative cycles of maximum likelihood refinement and manual model building reduced the R factor to 16.7% for all measured X-ray data from 30.0 to 1.62 Å resolution. The R free was 20.0% for 5% of the data that was excluded from the refinement. Refinement statistics are presented in Table 1. Analysis of the coordinates with the program PROCHECK (*10*) revealed that 92.5% of the residues lie in the most favored regions of the Ramachandran plot, whereas the remaining 7.5% of the residues lie in additionally allowed areas. No residues are located in the disallowed regions.

RESULTS AND DISCUSSION

The experiments described in this manuscript were designed to determine the functions of Lys 133 and Lys 235 in the OSBS-catalyzed reaction. Our hypothesis, based on previous structural studies of the Mg^{2+}·OSB complex and the location of C6 of the OSB product in the active site, was that Lys 235 would function as the catalytic base, and Lys 133 would function as the catalytic acid in an *anti* dehydration; it was hypothesized that mutagenesis of one or both of these residues would result in a catalytically impaired mutant that might be used for the determination of the structure of the Mg^{2+}·SHC complex.

Biosynthesis of SHCHC. Although this laboratory has described the enzymatic synthesis of SHCHC (Scheme 2), the absolute configuration of the carbon from which the proton is abstracted had not been determined (*4*). The synthesis of SHCHC is the first committed step in the menaquinone biosynthetic pathway. In vivo, isochorismate, the substrate for SHCHC synthase, is generated from chorismate by MenF, one of two homologous isochorismate synthases encoded by the *E. coli* genome. In our enzymatic synthesis, we utilized EntC, the second isochorismate synthase. The absolute configuration of isochorismate had been previously characterized, with no change in the absolute configuration of C2 (C6 in SHCHC), the OH-bearing carbon, occurring in the isochorismate mutase reaction. Conversion of isochorismate to SHCHC is an uncharacterized two-step process: the addition of the succinyl side chain derived from α-KG in a process using TDP followed by the elimination of pyruvate. In this reaction, the absolute configuration of C6 also is unchanged, but the absolute configuration of C1, the carbon from which the proton is abstracted in the OSBS-catalyzed reaction, has not been determined. In an attempt to resolve this uncertainty, we analyzed the ^{1}H NMR spectrum of SHCHC (data not shown) and realized that the coupling constants involving the protons of C1 and C6 (J5,6 = 5.5 Hz, J1,6 = 1.8 Hz) are consistent with either a cis or a *trans* relationship of the C1-carboxyl group and the C6-OH group. As a result, we have been unable to specify the stereochemical course of the OSBS-catalyzed reaction. However, because enzyme-catalyzed β-elimination reactions involving carboxylate anion substrates usually, but not always, proceed via an *anti* stereochemical course (*11*), we had assumed this stereochemical course and a *cis* relationship of the C1-carboxyl group and the C6-OH group. The structural studies reported in this paper resolve this ambiguity and demonstrate that this assumption is incorrect.

Kinetic Characterization of Mutant Enzymes. Six mutant enzymes were constructed and purified to homogeneity: K133A, K133S, K133R, K235A, K235S, and K235R. Using a spectrophotometeric assay, no detectable activity was observed for any of the mutants. The value of k_{cat} for each of the mutants was estimated as $< 3 \times 10^{-5}$ s^{-1} (the dehydration rate in the absence of enzyme), a 630 000-fold decrease from the value of 19 s^{-1} measured for wild-type OSBS.

Because the reactions catalyzed by members of the enolase superfamily are initiated by the abstraction of an α-proton to generate an enediolate anion intermediate, it was possible that the mutants might catalyze the exchange of the α-proton despite the lack of detectable dehydration activity (e.g., in a mechanism involving both a general base and a general acid, substitution of the general acid that facilitates the departure of the C6-OH group might allow the exchange of the α-proton without dehydration). Each mutant was separately incubated with SHCHC in D_2O, and both formation of the OSB product and exchange of the α-proton were monitored by ^{1}H NMR spectroscopy. Neither dehydration nor exchange of the α-proton was observed.

Effects of Mutations on the Circular Dichroism. CD spectra were obtained for wild-type OSBS and the six mutants to determine whether the mutations altered the secondary and tertiary structures. The spectra of the mutants were identical to those obtained for the wild-type enzyme (data not shown).

Active Site Structure. Crystals were obtained for the catalytically inactive K133R mutant protein in the presence of SHCHC. The electron density for the Mg^{2+}·SHCHC complex is essentially continuous for the entire length of the polypeptide chain with the exception of Arg 20, Ala 38, Pro 25, and Gly 126. The electron density starts at Met 1 and terminates at Leu 320. Likewise, almost all of the side chains are well-ordered (a list of disordered residues is given in Table 1).

The tertiary structure of the Mg^{2+}·SHCHC complex of the K133R mutant protein is essentially identical to that of the Mg^{2+}·OSB product complex of the wild-type enzyme described earlier. The rms difference between the positions of the α-carbon atoms is 0.30 Å for 306 residues. In contrast, the rms difference between the tertiary structure of the Mg^{2+}·SHCHC complex of the wild-type enzyme and the unliganded protein is 0.90 Å, where the larger difference is due to the rotation of the small domain relative to the (α/β)8 barrel when a ligand is present in the active site. This indicates that the domain movements associated with the active site closure are similar regardless of whether the substrate or product are bound.

The electron density for the K133R mutation shows that, in contrast to the earlier structures where the Lys 133 extended toward the putative location of C1 in the substrate, the side chain for arginine extends to the solvent, where the electron density suggests that the side chain is quite mobile (Figure 1). The displacement of the arginine side chain from the active site is consistent with the increased size and polarity of the guanidinium moiety as compared to the amino group of lysine.

Examination of the active site reveals the electron density for a well-ordered molecule of SHCHC (Figure 2). This unequivocally defines the stereochemistry of the substrate and shows that the C1-carboxylate and the C6-OH leaving group have a *trans* orientation, and the absolute configurations of both carbons are *R*. The absolute configuration of C1 differs from that assumed in the earlier structural studies of the wild-type enzyme, which leads directly to a different assignment for the catalytic acid and base as discussed below.

The C1 carboxylate of SHCHC forms a bidentate interaction with the magnesium ion. The remainder of the coordination sphere of the magnesium ion is completed by monodentate interactions with the carboxylates of Asp 161, Glu 190, and Asp 213 and a water molecule. All of the bond distances to the magnesium ion lie in the range of 1.9−2.1 Å, which is consistent with normal geometry for this ion
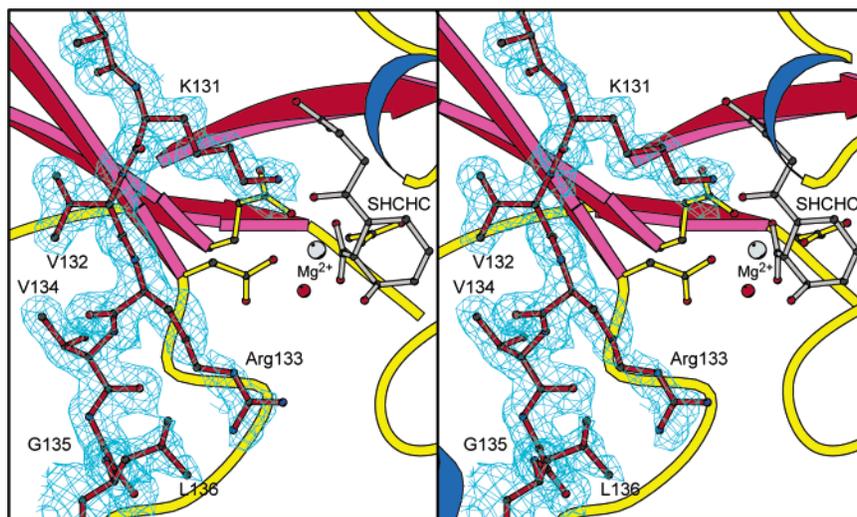
FIGURE 1: Stereoview of the electron density for Ala 130−Leu 136 and its proximity to SHCHC. This figure reveals that the side chain of Arg 133 (mutational change K133R relative to the wild-type enzyme) extends away from C1 of the substrate toward the solvent. The map was calculated with coefficients of the form $2F_o − F_c$ and was contoured at 1 σ. Figures 2−6 were prepared with the programs Molscript and Bobscript (*12, 13*).

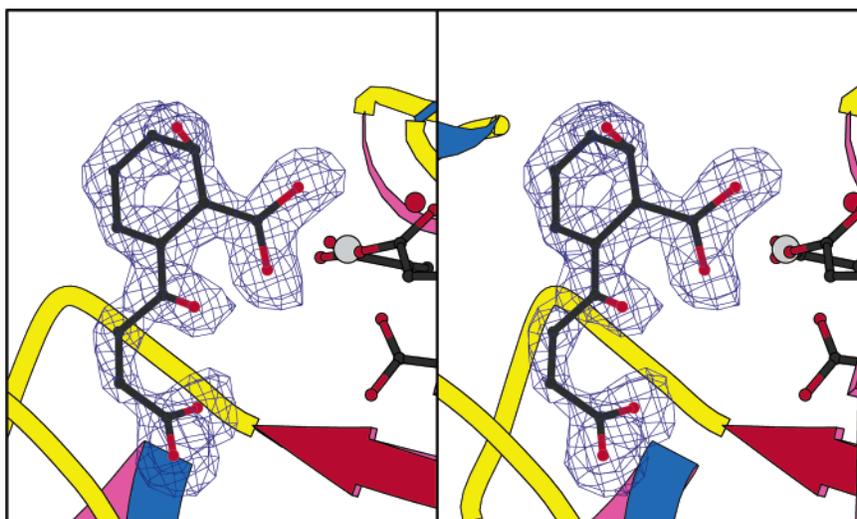

FIGURE 2: Stereoview of electron density for SHCHC. The map was calculated with coefficients of the form $F_o − F_c$ and was contoured at 3 σ where the substrate was omitted from the phase calculation. This shows that the conformation of SHCHC is unequivocally 1*R*,6*R* where the C1 carboxylate and C6−OH leaving group are in the *trans* configuration.

(Figure 3A). The overall coordination of the magnesium ion can be described as distorted octahedral.

The arrangement of ligands around the magnesium ion in the complex with SHCHC is different from that observed in the complex with OSB. In the latter case, OSB only utilized a single interaction between a carboxylate oxygen and the magnesium ion (*3*). This results in a different position for SHCHC and OSB in the active site (Figure 4) and is expected based on the change in hybridization at C1 and C6 from sp^3 to sp^2. Because of the movement of the carboxylate on C1 into the plane of the aromatic ring, the metal coordination of the carboxylate changes from bidentate in SHCHC to monodentate in OSB. This results in a translation of the remainder of the molecule by approximately 0.8 Å. This change allows the hydrophobic component of the substrate and product to remain in approximately the same plane. Apart from the change in the configuration of C1, the overall arrangement of atoms in both the substrate and the product are very similar. The movement of the product relative to the substrate requires only a minor rearrangement of the side

chains in contact with the ligands (data not shown) so that ligand interaction diagram is essentially identical to that described earlier (*3*). Interestingly, the movement of the succinyl carboxylate group of SHCHC relative to that in OSB is accompanied by a rotation of the ϵ-amino group of Lys 131, which serves to maintain an ionic interaction that stabilizes both substrate and product complex. A shift of ∼0.8 Å between substrate and product is readily accommodated by nonpolar interactions, whereas such a movement would be highly unfavorable for an ionic interaction without a compensatory change.

Structural Mechanism. The kinetic effects of mutations at Lys 133 and Lys 235 in combination with the structure of the K133R mutant in the presence of SHC support a mechanism in which Lys 133 serves as the catalytic base for the initial proton abstraction event as depicted in Figure 5. The orientation of the C6 hydroxyl suggests that Lys 133 also serves as the catalytic acid responsible for protonation of the departing water molecule. Lys 235, although essential for enzyme activity, is on the opposite side of substrate and
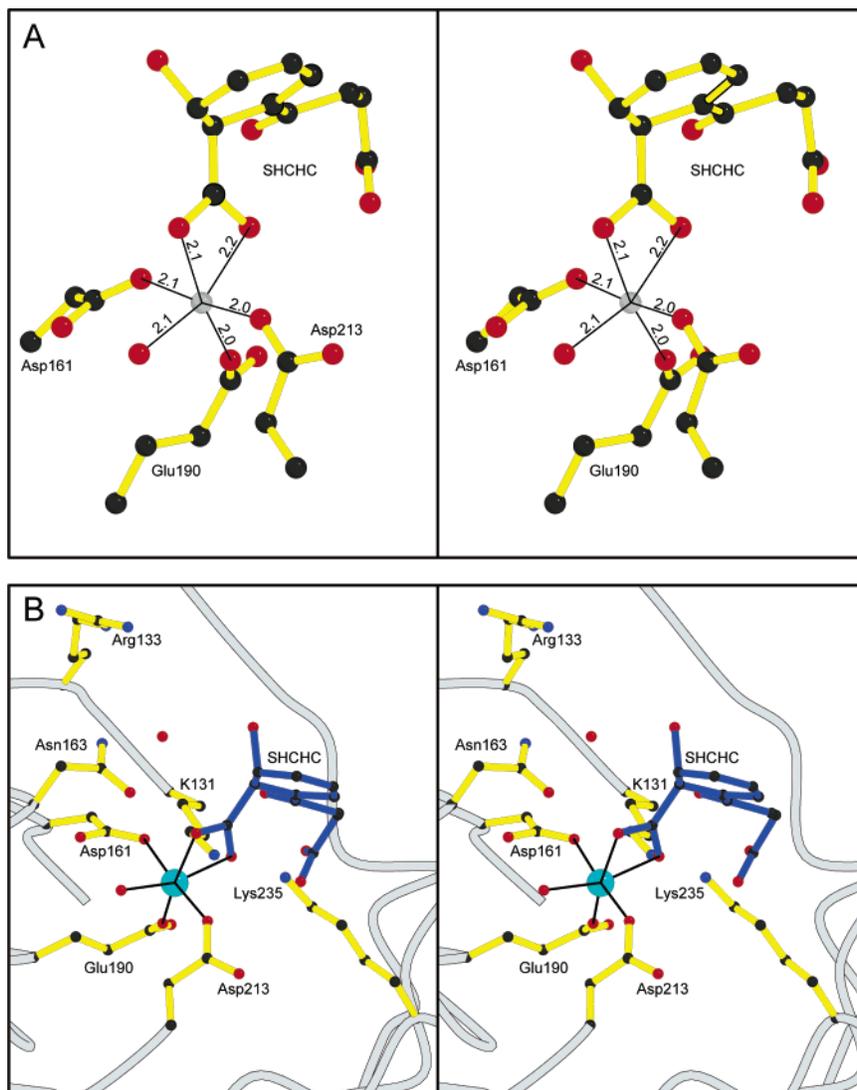
FIGURE 3: Stereoviews of the active site for and its coordination of SHCHC. Panel A shows the geometry of the metal coordination site, which is approximately octahedral with its associated bond distances. Panel B shows the ligand interactions of SHCHC with *o*-succinylbenzoate synthase. This illustrates that Lys 235 is on the opposite side to the proton that is abstracted by Lys 133 and the C6−OH leaving group and thus cannot function as either the catalytic base or the acid.
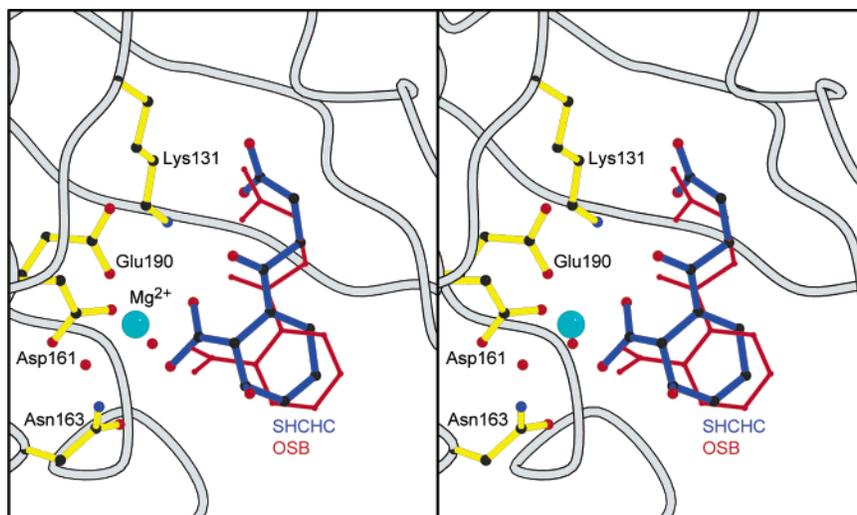

FIGURE 4: Stereo overlap of SHC in the K133R mutant protein and OSB in the wild-type structure (*3*). The coordinates for the product complex were taken from the RSCB with accession number 1FHV and superimposed with the program Align (*14*).
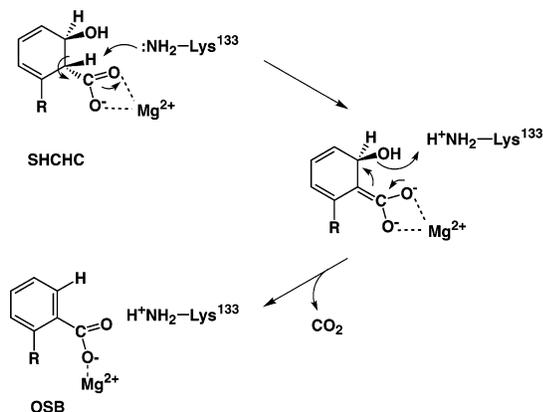
FIGURE 5: Revised mechanism for the *o*-succinylbenzoate synthase-catalyzed reaction.

is unable to abstract the proton as indicated by the stereochemistry of C1. Given its position, Lys 235 may stabilize the negative charge on the enediolate intermediate through a cation−π interaction (Figure 3B). The inability of substitutions for Lys 235 to catalyze either dehydration or exchange of the α-proton can be explained by the loss of this stablizing interaction.

This mechanism is different from that proposed earlier on the basis of the structure of the OSB product complex (*3*). In that work, Lys 235 was proposed to be the catalytic base, whereas Lys 133 was projected to function as the catalytic acid. This proposal was derived based on the position of OSB, at a time when the absolute configuration of the substrate was unknown, so that the only constraint was the position of C1 and C6. The suggestion that Lys 133 would serve as the required base and Lys 235 would function as the acid seemed entirely acceptable given the conservation and function of these residues in the MLE subgroup of the enolase superfamily. However, it is now realized that, like the *syn* dehydration catalyzed by (D)-glucarate dehydratase (GlucD), a single residue can catalyze both proton abstraction and departure of the leaving group. In GlucD, a member of the MR subgroup, His 339 at the end of the seventh β-strand is the dual function catalyst.

CONCLUSIONS

This study provides a structural mechanism for the reaction catalyzed by the OSBS from *E. coli*, which is expected to

apply to all orthologs. Importantly, Lys 133 serves both as the catalytic base and as the acid, whereas the conserved Lys 235 that lies on the opposite side of the substrate appears to provide a positive charge that stabilizes the enediolate intermediate. Such assistance in catalysis is a new function for an active site functional group in the enolase superfamily, thereby expanding the potential catalytic functions of conserved active site residues in the enolase superfamily. The present studies highlight the importance of high-resolution structural studies of enzyme−substrate complexes, to both define the geometry of the bound substrate and to identify the roles of individual residues. Finally, this study illustrates the difficulty of assigning functions to individual residues based on the structure of a complex with a product that differs significantly in both structure and energy from the transition state.

REFERENCES

1. Babbitt, P. C., Hasson, M. S., Wedekind, J. E., Palmer, D. R., Barrett, W. C., Reed, G. H., Rayment, I., Ringe, D., Kenyon, G. L., and Gerlt, J. A. (1996) *Biochemistry 35*, 16489−501.
2. Meganathan, R. (1996) in *Escherichia coli and Salmonella: Cellular and Molecular Biology* (Neidhart, F. C., Curtis, R., Ingraham, J. L., Lin, E. C. C., Low, K. B., Magasanik, B., Reznikoff, W. S., Riley, M., Schaechter, M., and Umbarger, H. E., Eds.) pp 642−656, ASM Press, Washington, DC.
3. Thompson, T. B., Garrett, J. B., Taylor, E. A., Meganathan, R., Gerlt, J. A., and Rayment, I. (2000) *Biochemistry 39*, 10662−76.
4. Palmer, D. R., Garrett, J. B., Sharma, V., Meganathan, R., Babbitt, P. C., and Gerlt, J. A. (1999) *Biochemistry 38*, 4252−8.
5. Rayment, I. (2002) *Structure 10*, 147−51.
6. Otwinowski, Z., and Minor, W. (1997) *Methods Enzymol. 276*, 307−26.
7. CCP4 (1994) *Acta Crystallogr. D50*, 760−3.
8. Murshudov, G. N., Vagin, A. A., and Dodson, E. J. (1997) *Acta Crystallogr. D53*, 240−255.
9. Perrakis, A., Harkiolaki, M., Wilson, K. S., and Lamzin, V. S. (2001) *Acta Crystallogr. D57*, 1445−50.
10. Laskowski, R. A., MacArthur, M. W., Moss, D. S., and Thornton, J. M. (1993) *J. Appl. Crystallogr. 26*, 283−91.
11. Palmer, D. R. J., Wieczorek, S. J., Hubbard, B. K., Mrachko, G. T., and Gerlt, J. A. (1997) *J. Am. Chem. Soc. 119*, 9580−1.
12. Kraulis, P. J. (1991) *J. Appl. Crystallogr. 24*, 946−50.
13. Esnouf, R. M. (1999) *Acta Crystallogr. D55*, 938−40.
14. Cohen, G. H. (1997) *J. Appl. Crystallogr. 30*, 1160−1.